Surface plasmon resonance and photoluminescence studies of Au and Ag micro-flowers

R. Zakaria,[1,2]* K.S. Hamdan,[2] S.M. Che Noh,[2] A. Supangat[3] and M. Sookhakian[2]

[1]*Photonics Research Centre, Faculty of Science, University of Malaya, 50603 Kuala Lumpur, Malaysia*
[2]*Physics Department, Faculty of Science, University of Malaya, 50603 Kuala Lumpur, Malaysia*
[3]*Low Dimensional Materials Research Centre, Faculty of Science, University of Malaya, 50603 Kuala Lumpur, Malaysia*
*rozalina@um.edu.my

Abstract: The surface plasmon resonance (SPR) and photoluminescence characteristics of gold and silver micro-flowers were compared to those of gold and silver nanoparticles. The micro-flower structures were grown under electron beam deposition using an alumina template. Both types of metallic micro-flowers showed systematic arrangements; they formed islands of flowers about 20 μm across, each one comprised of spikes ranging from 1 to 5 μm in length. A red shift in the SPR and enhancement intensity was observed for both micro-flowers and nanoparticles; the incremental increase was more than 50%. These results, which showed that gold and silver micro-flowers agglomerate at a micron size scale, are useful for the design of easier and more cost effective methods for large area fabrication, especially for particular plasmonic applications.

OCIS codes: (160.4236) Nanomaterials; (160.4670) Optical materials; (160.4760) Optical properties; (220.4610) Optical fabrication; (220.4241) Nanostructure fabrication.

References and links

1. F. Bohren, "How can a particle absorb more than the light incident on it?" Am. J. Phys. **51**(4), 323–327 (1983).
2. L. Shao, A. S. Susha, L. S. Cheung, T. K. Sau, A. L. Rogach, and J. Wang, "Plasmonic properties of single multispiked gold nanostars: Correlating modeling with experiments," Langmuir **28**(24), 8979–8984 (2012).
3. S. M. Huang, Z. Sun, and Y. F. Lu, "Nanofabrication by laser irradiation of polystyrene particle layers on silicon," Nanotechnology **18**, 025302, (2007).
4. N. Murphy-DuBay, L. Wang, E. C. Kinzel, S. M. V. Uppuluri, and X. Xu, "Nanopatterning using nsom probes integrated with high transmission nanoscale bowtie aperture," Opt. Express **16**(4), 2584–2589 (2008).
5. A. Khan, Z. Wang, M. A. Sheikh, D. J. Whitehead, and L. Li, "Laser micro/nano patterning of hydrophobic surface by contact particle lens array," Appl. Surf. Sci. **258**(2), 774–779 (2011).
6. L. Pan, Y. Park, Y. Xiong, E. Ulin-Avila, Y. Wang, L. Zeng, S. Xiong, J. Rho, C. Sun, D. B. Bogy, and X. Zhang, "Maskless plasmonic lithography at 22 nm resolution," Sci Rep **1**(175), 175 (2011).
7. J. Grunes, J. Zhu, E. A. Anderson, and G. A. Somorjai, "Ethylene hydrogenation over platinum nanoparticle array model catalysts fabricated by electron beam lithography: Determination of active metal surface area," J. Phys. Chem. B **106**(44), 11463–11468 (2002).
8. S. Biring, "Tuning of particle resonances in binary dielectric medium," Phys. Lett. A **376**(2), 125–127 (2011).
9. M.-C. Wu, M.-P. Lin, S.-W. Chen, P.-H. Lee, J.-H. Li, and W.-F. Su, "Surface-enhanced raman scattering substrate based on ag coated monolayer sphere array of sio2 for organic dye detecting," RSC Advances, 2013.
10. B. I. Kharisov, "A review for synthesis of nanoflowers," Recent Pat. Nanotechnol. **2**(3), 190–200 (2008).
11. Y. Jiang, X.-J. Wu, Q. Li, J. Li, and D. Xu, "Facile synthesis of gold nanoflowers with high surface-enhanced Raman scattering activity," Nanotechnology **22**(38), 385601 (2011).
12. G. T. Boyd, Z. H. Yu, and Y. R. Shen, "Photoinduced luminescence from the noble metals and its enhancement on roughened surfaces," Phys. Rev. B Condens. Matter **33**(12), 7923–7936 (1986).
13. O. A. Yeshchenko, I. M. Dmitruk, A. A. Alexeenko, M. Y. Losytskyy, A. V. Kotko, and A. O. Pinchuk, "Size-dependent surface-plasmon-enhanced photoluminescence from silver nanoparticles embedded in silica," Phys. Rev. B **79**(23), 235438 (2009).
14. X. T. Zhang, K. M. Ip, Q. Li, and S. K. Hark, "Photoluminescence of ag-doped znse nanowires synthesized by metalorganic chemical vapor deposition," Appl. Phys. Lett. **86**(20), 203114 (2005).

15. V. Giannini, R. Rodríguez-Oliveros, and J. A. Sánchez-Gil, "Surface plasmon resonances of metallic nanostars/nanoflowers for surface-enhanced raman scattering," Plasmonics **5**(1), 99–104 (2010).
16. R. Bardhan, N. K. Grady, J. R. Cole, A. Joshi, and N. J. Halas, "Fluorescence enhancement by au nanostructures: Nanoshells and nanorods," ACS Nano **3**(3), 744–752 (2009).
17. B. D. Liu, Y. Bando, C. C. Tang, D. Golberg, R. G. Xie, and T. Sekiguchi, "Synthesis and optical study of crystalline gap nanoflowers," Appl. Phys. Lett. **86**(8), 083107 (2005).
18. S. Link and M. A. El-Sayed, "Size and temperature dependence of the plasmon absorption of colloidal gold nanoparticles," J. Phys. Chem. B **103**(21), 4212–4217 (1999).
19. J. S. T. Smalley, Q. Gu, and Y. Fainman, "Temperature dependence of the spontaneous emission factor in subwavelength semiconductor lasers," IEEE J. Quantum Electron. **50**(3), 175–185 (2014).
20. S. K. Özdemir and G. Turhan-Sayan, "Temperature effects on surface plasmon resonance: Design considerations for an optical temperature sensor," J. Lighw. Tech. **21**(3), 805–814 (2003).
21. K. S. Hamdan, S. M. Abdullah, K. Sulaiman, and R. Zakaria, "Effects of silver nanoparticles towards the efficiency of organic solar cells," Appl. Phys., A Mater. Sci. Process. **115**(1), 63–68 (2014).
22. G. A. Wurtz, W. Dickson, D. O'Connor, R. Atkinson, W. Hendren, P. Evans, R. Pollard, and A. V. Zayats, "Guided plasmonic modes in nanorod assemblies: Strong electromagnetic coupling regime," Opt. Express **16**(10), 7460–7470 (2008).
23. S. Ye, Y. Hou, R. Zhu, S. Gu, J. Wang, Z. Zhang, S. Shi, and J. Du, "Synthesis and photoluminescence enhancement of silver nanoparticles decorated porous anodic alumina," J. Mater. Sci. Technol. **27**(2), 165–169 (2011).
24. M. B. Mohamed, V. Volkov, S. Link, and M. A. El-Sayed, "The `lightning' gold nanorods: Fluorescence enhancement of over a million compared to the gold metal," Chem. Phys. Lett. **317**(6), 517–523 (2000).
25. Y. Zhao, Y. Jiang, and Y. Fang, "Spectroscopy property of ag nanoparticles," Spectrochim. Acta A Mol. Biomol. Spectrosc. **65**(5), 1003–1006 (2006).
26. T. Suna, Z. Xua, W. Zhaoa, X. Wua, S. Liua, Z. Zhanga, S. Wanga, W. Liua, S. Liub, and J. Peng, "Fabrication of the similar porous alumina silicon template for soft uv nanoimprint lithography," Appl. Surf. Sci. **276**, 363–368 (2013).
27. H. Hu, H. Duan, J. K. W. Yang, and Z. X. Shen, "Plasmon-modulated photoluminescence of individual gold nanostructures," ACS Nano **6**(11), 10147–10155 (2012).

Introduction

Plasmonic properties of metallic nanoparticles have been extensively studied because of their unique optical properties such as resonant absorption and light scattering [1]. These coherent oscillations, also known as surface plasmon resonance (SPR), lead to an enhanced local electric field in the vicinity of the surface of the particles that is highly shape and size-dependent. The synthesis of metal nanoparticles is gradually shifting from the traditional spherical shaped nanoparticles to progressively more complex shapes, such as anisotropic and branched particles [2]. The creation of these different shapes appears to be an effective strategy for tuning SPR properties of gold (Au) and silver (Ag) nanoparticles. Researchers have employed various fabrication techniques to study different shapes and structures in order to optimise the SPR properties of these structures. Some of these fabrication techniques are laser-induced surface patterning [3], NSOM patterning [4], contacting particle-lens array [5], plasmonic lithography [6], electron beam lithography [7] and various hard template methods such as the use of alumina templates [8], polystyrene [3] and SiO_2 sphere monolayer [9] colloidal crystals. Among these fabrication techniques, hard-template methods have been widely used because of their simplicity, and cost effective method. Variety of Ag nanostructures such as rose-, spike-, and snowflake-shapes have been successfully synthesized mostly by using wet method like reduces silver nitrate [10] in chemical solutions.

Many fascinating studies have used noble metal nanostructures to examine surface-enhanced Raman scattering [11] and surface enhanced fluorescence [12]. These studies have been focused on the electromagnetic enhancement at so-called 'hot spots' in the vicinity of nanoparticles. The efficacy of the resonant effect has been observed in the photoluminescence of Au, Ag and copper and with it several orders of magnitude larger in bulk films [13]. Experimental measurements [14] and theoretical calculations [15] have shown that 'hot-spots' in individual structures can enhance the electromagnetic fields of complex metallic nanostructures, for example dendrites, multi-pods and nanoflowers. Metallic nanoparticles have been shown to enhance the fluorescence emission and decrease the molecular excited-state lifetimes of vicinal fluorophores. These effects are attributable to a combination process involving enhanced absorption by the molecule, coupling efficiency and fluorescent emission [16].

This letter presents some results from comparative studies of the SPR and photoluminescence properties of Au and Ag micro-flowers with those of Au and Ag nanoparticles. Spherical nanoparticles were formed using electron beam evaporation, whereby alumina template was attached on the substrate to produce micro-flowers using the same technique. Studying absorption and fluorescence enhancement of these two types of structures allowed us to investigate by virtue the properties of both structures contribute to this effect. The results showed that Au and Ag micro-flowers contributed up to 50% of the enhancement of the absorption and photoluminescence properties of the Au and Ag nanoparticles.

Experimental method

Thin layers of Au and Ag were firstly deposited on ITO-coated glass substrates using electron beam evaporation techniques with a high vacuum chamber of 2 x 10^{-5} mbar. These deposited samples were then been annealed for 2 hours at 400°C and 250°C for Au and Ag, respectively. The deposited Au and Ag produced a nanosize (10-20 nm) spherical particle and they were distributed uniformly and spherically on the substrate.

Anodic aluminum oxide (AAO) template with nominal pore diameter of 20 nm and thickness of 60 μm was purchased from Whatman Anodisc Inorganic Membrane (Sigma-Aldrich, St. Louis, MO, USA) were used in this process. Notably, the commercial template (Whatman) exhibits the branched structure throughout the template which may support to the preceding observation. The templates were cleaned prior to use by sonication in water and acetone for 15 minutes. The deposition process used electron beam evaporation to obtain structures of Au and Ag that fit the mould of the alumina template. The micro-flowers grew within the template pores and then, after the template was inverted, they stuck to the copper tape; thus, they had an upside down formation. After this process, the alumina template was dissolved in a 3M sodium hydroxide solution and rinsed thoroughly with deionised water until the pH of the solution became neutral. These micro-flowers were characterised using field emission scanning electron microscopy (FESEM) (Quanta FEG 450), UV-Vis spectroscopy (Shimadzu UV-3101PC) and photoluminescence spectroscopy (RENISHAW).

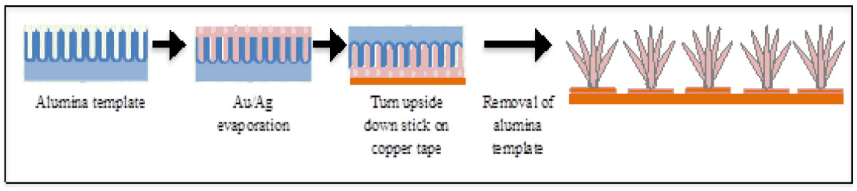

Fig. 1. Schematic diagram of the fabrication of Au/Ag micro-flowers.

Figure 1 shows the schematic diagram of the fabrication of Au and Ag micro-flowers using alumina template. First, the Au and Ag were deposited on the template using electron beam evaporation, then the whole template was rotated 180°, causing the structures to adhere to the copper tape. Then the template was dissolved in a NaOH solution for 24 hours.

Results and discussions

The morphological structures of the Au and Ag were observed physically using FESEM. Figures 2 and 3 show the micro-flower formation of Au and Ag respectively, while those of the spherical nanoparticles structures are shown in Fig. 5(a) and 5(b).

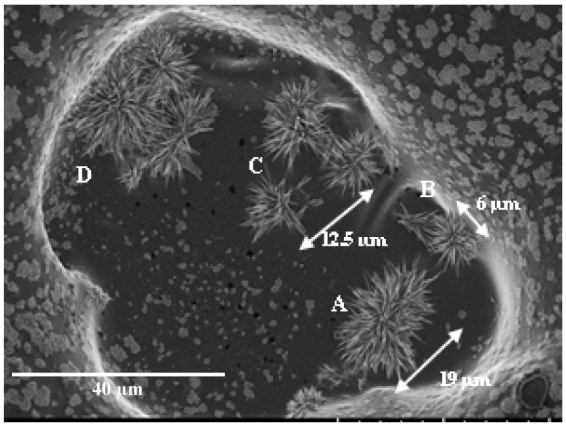

(a)

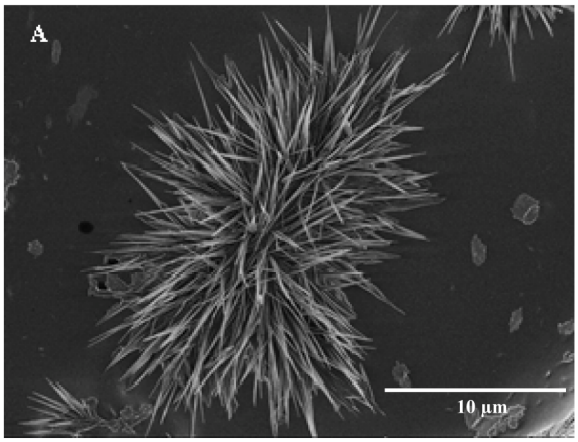

(b)

Fig. 2. FESEM images of (a) several clusters of Au micro-flowers at the selected area with sizes and spacing shown under low magnification, revealing the size of micro-flowers as small as ~6 µm and (b) a cluster from area A in 2(a), shown at higher magnification.

Figure 2(a) shows FESEM image of Au micro-flowers with some notable features as follows: (A) is a cluster of Au micro-flowers of ~19 µm; (B) is a single Au island approximately 6 µm in size; and (C) is an island of Au micro-flowers that formed in a more systematic arrangement with a spacing of ~12.5 µm. Figure 2(b) is an extracted image from Fig. 2(a) that shows (A) at a higher magnification. The mean length of the spikes in this formation was found to be smaller than template size, with ranging from ~1.5 µm to ~5 µm. The diameter of each spike varied over its length by as much as 0.5 µm. These formations do not appear to match the template's diameter, perhaps due to agglomeration during deposition and removal process. The thickness of the film which consists the micro-flowers is measured to be ~10 µm, this is most probably due to insufficient penetration in the pores using dry deposition technique.

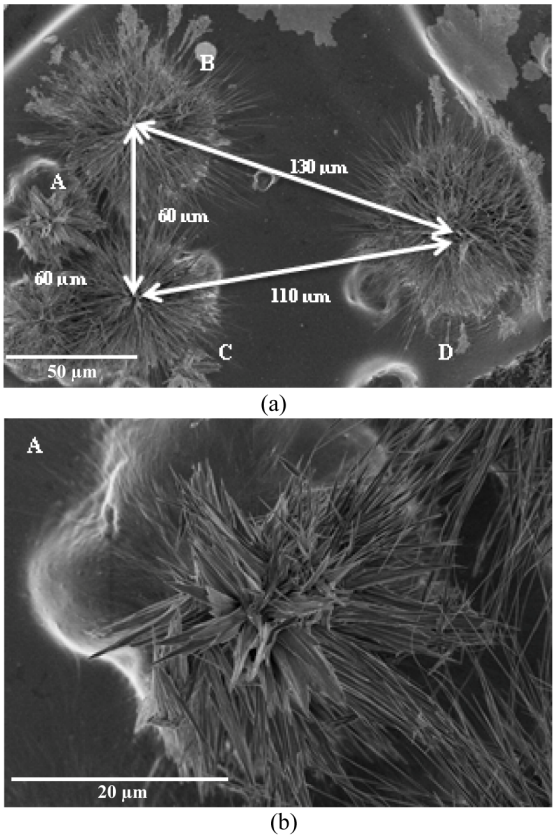

Fig. 3. FESEM images of (a) several clusters of Ag micro-flowers at the selected area with sizes and spacing stated, with the smallest formation measured about 60 µm and (b) a cluster from area A in Fig. 3(a) at a higher magnification.

Figure 4 compares the absorption spectrum of the metallic micro-flowers with the nanoparticles structures. For all of the spectra shown, an analogically treated and non-activated substrate was defined as a reference and was subtracted from the UV-Vis spectra of the measured structures. Figure 4(a) depicts the trend between the Au micro-flowers (black line) and Au nanoparticles (red line); this scattering spectra of Au nanoparticles showed that the localised SPR occurred at 545 nm with an absorbance of 0.3. The absorption spectra of the Au micro-flowers shifted slightly to a red-shift at the maximum peak of 560 nm with an absorbance of 0.57. This experimentally observed SPR wavelength red-shift for the micro-flowers was expected due to some impurity effects [17] such as atomic vacancies on the flower surface rather than due to the increasing size of the flower structures. Indeed, both resonances (for Au and Ag micro-flowers) are red-shifted because of their intrinsic properties results from hybridization of plasmons focalized at the core and tips of the structures [15]. This structure acts as antenna producing electromagnetic field enhancements of the tip plasmons and the morphology of the spikes (length and aperture angle). Their number of petals are also contributes to strong effect of plasmon frequency and intensity. The bandwidth was broader in the size region above 20 nm [18], probably because the frequency depended on the dielectric function of the particles. Due to the anisotropic shape of the Au micro-flowers, they displayed two separate SPR bands, corresponding to their width and length; these are known as the transverse SPR (TSPR) and longitudinal SPR bands (LSPR). The calculated enhancement was up to 47% increase, indicating that the morphology of the micro-flowers potentially contributed to the higher absorption because of the multi-spikes and irregularity formed in each micro-flower.

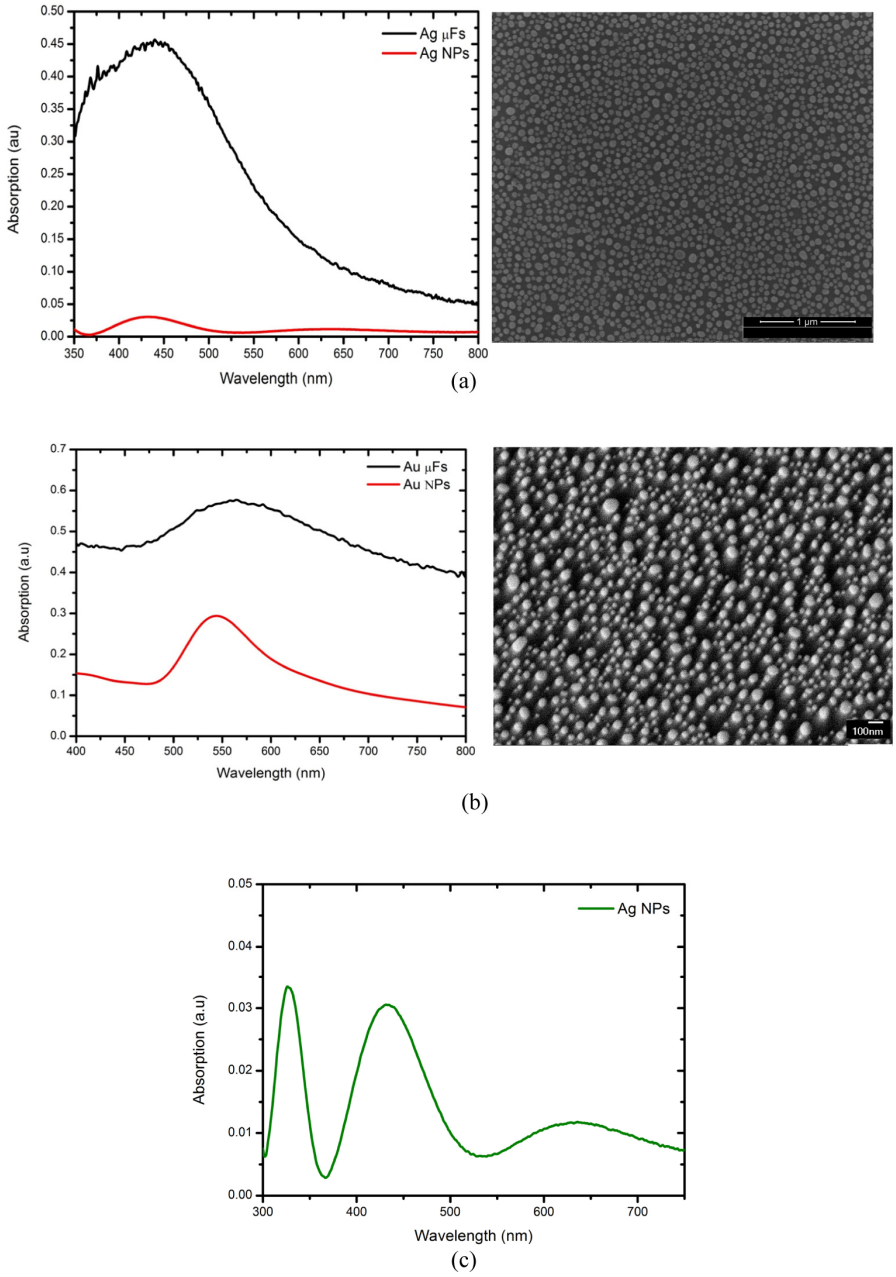

Fig. 4. UV-Vis absorption spectra comparing (a) Au micro-flowers and Au nanoparticles with an FESEM image of Au nanoparticles which had an even distribution of ~20nm and (b) Ag micro-flowers, the band shown is between 545 nm and 440 nm, which is the transverse plasmon resonance. An FESEM image of the Ag nanoparticles is also shown. c) UV-vis absorption spectra for Ag nanoparticles.

Comparison of UV-Vis absorption spectra between Ag micro-flowers and the Ag nanoparticles is presented in Fig. 4(b). Both had shown similar trend at a low wavelength (< 500 nm). The Ag micro-flowers had a stronger peak maximum at 440 nm and gradually decreased with the longer wavelengths. Whereas the Ag nanoparticles graph

shows an SPR band in the 300-750 nm range, with an absorption peak at 445 nm (TSPR band) and a broader peak at 645 nm (LSPR).

The FESEM images, shown in Figs. 4(a) and 4(b), demonstrate growth in both the Au and Ag nanoparticles after thermal annealing at 400°C and 250°C, respectively. It has been previously demonstrated, theoretically [19] and experimentally [20], that thermal conditions play a role in the SPR and luminescence of plasmonic structures. However, the formation of Au and Ag nanoparticles reported here occurred at specific annealing temperatures. The size of the spherical Ag nanoparticles (~20 nm) and the inter-particle distances were similar [21], perhaps due to the coherent coupling between molecular excitons and the electronic polarisations of noble metal nanoparticles. The effects of resonant coupling as a function of spectral overlap were experimentally reported by Wurtz et al. [22], who used J-aggregate molecules on nanowire assemblies with tunable LSPR. This comparison gives the enhancement value as high as ~89% for Ag micro-flowers relative to the Ag nanoparticle structure at 440 nm.

To study the influence of photoluminescence, spectra were acquired under excitation from a frequency-doubled neodymium-doped yttrium aluminium garnet laser operating at λ_{exc} = 532 nm focus through 10 x microscopy objective (NA = 0.8) at normal incidence. In the comparison of the photoluminescence of the Au and Ag micro-flowers with that of the Au and Ag nanoparticles, the fluorescence enhancement should be attributed to the metal enhancement effect [23]. The field enhancement can affect the spontaneous decay rate and PL intensity. According to theoretical studies of photo induced luminescence, a single-photon luminescence power P_1 can be calculated for the excitation and emission energies $h\omega_{exc}$ and $h\omega_{em}$ using the following equation [24]:

$$P_1 = 2^4 \beta_1 \left|E_0\right|^2 V \left|L^2(\omega_{exc}) L^2(\omega_{em})\right|, \quad (1)$$

where E_0 is the incident electric field and β_1 is the proportionality constant, which includes the intrinsic luminescence spectrum of the metallic compound. The resonant luminescence power increases with increasing nanorod [24] length to a longer emission wavelength.

Note that the PL spectra presented in Fig. 5 were obtained by subtracting the substrates used (ITO for the nanoparticles and copper tape for the micro-flowers). This graph shows that, in general, the intensity of the Au micro-flowers was higher than that of the Ag micro-flowers, but it shows the opposite pattern for the photoluminescence spectrum of the Au and Ag nanoparticles. The visible luminescence of Au/Ag is caused by the excitation of electrons from occupied *d* bands into states above the Fermi level. The subsequent electron-phonon and hole-phonon scattering process leads to an energy loss and finally to the PL radiative recombination of electrons from an occupied *sp* band with the hole [25].

The Au micro-flowers had clearly higher photoluminescence than the Au nanoparticles. However, the Ag nanoparticles had a higher intensity than the Ag micro-flowers emission spectra in the 800 nm wavelength range. Table 1 gives the detailed peak values at particular wavelengths. The Peak (I) for the Au micro-flowers was 600 nm with PL_{max} = 38026, and the Au nanoparticles Peak (I) was 716 nm with PLmax as 16676; the photoluminescence value of these nanostructures was twice that of the micro-flowers. However, Peak (I) of the Ag micro-flowers was 591 nm (PL_{max} = 5341) and the peak of the Ag nanoparticles at this wavelength gave a PL value of 7692. In this case, the photoluminescence values were 1.44 times higher for the Ag nanoparticles than for the Ag micro-flowers. This higher emission has been attributed to an oxide-originated defect rather than to the size of the confinement effect [26]. Ag is known to be easily oxidised due to the high content of Ag in the particles' inner core. Specifically, in the comparison of the Au and Ag micro-flowers, the PL intensity of Au was eight times higher than that of Ag. At an excitation of 532 nm, the Au micro-flowers PL peak appearing at 603 nm was slightly lower than that of the Au nanorod at 653 nm reported by Hailong Hu et. al. [27]

Table 1. Comparison of Wavelength and Photoluminescence Maximum of Au/Ag micro-flowers (μF) and Au/Ag nanoparticles (NP)

	Au μF		Au NP	Ag μF		Ag NP	
	Peak I	Peak II	Peak I	Peak I	Peak II	Peak I	Peak II
Wavelength (nm)	600	1159	716	591	1175	591	780
PL (max)	38026	47402	16676	5341	15108	7692	31523

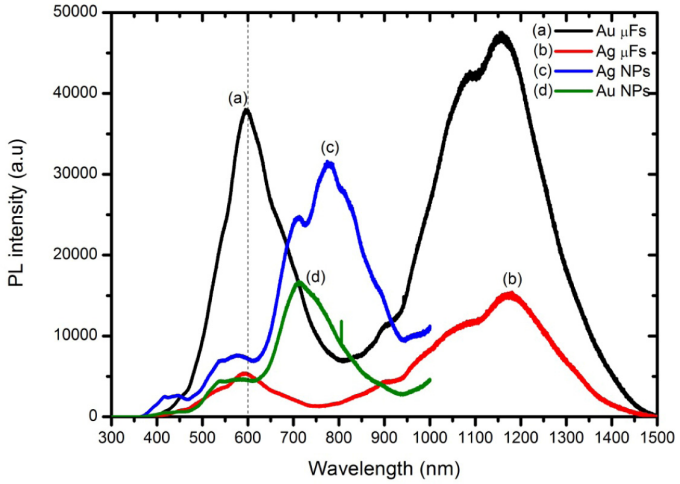

Fig. 5. Photoluminescence spectrum analysis comparing of Au/Ag micro-flowers (μF) and Au/Ag nanoparticles (NP). Unlike the Au/Ag nanoparticles, the Au micro-flowers had a higher intensity than the Ag micro-flowers.

Conclusions

In this work, the resultant micro-flowers shapes displayed a considerable enhancement effect in both absorption and photoluminescence analysis compared to spherical structures. We have shown that such metal micro-flowers exhibit strong absorption spectra with a main SPR red-shifted in comparison with spherical structures. This is due to the morphology of the flower-like structures occurring at the interstices in between petals occupy larger areas and yield larger field enhancement factors. However, this fabrication method still needs to be optimised for more uniformity distribution.

Acknowledgments

The work was supported by the University Malaya Research Grants RU 001-2014 and RP008E-13AET.